The EMBO Journal (2008) 27, 606–617 | © 2008 European Molecular Biology Organization | All Rights Reserved 0261-4189/08
www.embojournal.org

THE
EMBO
JOURNAL

WGEF activates Rho in the Wnt–PCP pathway and controls convergent extension in *Xenopus* gastrulation

Kosuke Tanegashima, Hui Zhao and Igor B Dawid*

Laboratory of Molecular Genetics, National Institute of Child Health and Human Development, National Institutes of Health, Bethesda, MD, USA

The Wnt–PCP (planar cell polarity, PCP) pathway regulates cell polarity and convergent extension movements during axis formation in vertebrates by activation of Rho and Rac, leading to the re-organization of the actin cytoskeleton. Rho and Rac activation require guanine nucleotide-exchange factors (GEFs), but the identity of the GEF involved in Wnt–PCP-mediated convergent extension is unknown. Here we report the identification of the weak-similarity GEF (*WGEF*) gene by a microarray-based screen for notochord enriched genes, and show that WGEF is involved in Wnt-regulated convergent extension. Overexpression of *WGEF* activated RhoA and rescued the suppression of convergent extension by dominant-negative Wnt-11, whereas depletion of *WGEF* led to suppression of convergent extension that could be rescued by RhoA or Rho-associated kinase activation. WGEF protein preferentially localized at the plasma membrane, and Frizzled-7 induced colocalization of Dishevelled and WGEF. WGEF protein can bind to Dishevelled and Daam-1, and deletion of the Dishevelled-binding domain generates a hyperactive from of WGEF. These results indicate that WGEF is a component of the Wnt–PCP pathway that connects Dishevelled to Rho activation.

The EMBO Journal (2008) **27,** 606–617. doi:10.1038/emboj.2008.9; Published online 7 February 2008
Subject Categories: signal transduction; development
Keywords: convergent extension; gastrulation; GEF; Wnt–PCP; *Xenopus*

Introduction

During vertebrate development, distinct cellular behaviours control the extension of the anterior–posterior axis through cell movements called convergent extension (CE). CE occurs in dorsal mesoderm and neural ectoderm to narrow the width of these tissues and extend their length along the anterior–posterior axis, thereby generating the basic body plan of the vertebrate animal. Impairment of CE is a causative factor for certain neural tube-closure defects, one of the common human birth defects occurring in 1 out of every 1000 births (Copp *et al*, 2003). CE in *Xenopus* involves cellular rearrangements through changes in cell morphology and the elaboration of cytoplasmic protrusions (Shih and Keller, 1992; Keller, 2002; Wallingford *et al*, 2002). Protrusive activity generates traction on the neighbouring cells to promote cell intercalation that is a hallmark of the CE process (Keller and Jansa, 1992). Dorsal mesodermal cells exhibit actively extending and retracting lamellipodia that contain actin-rich structures (Kwan and Kirschner, 2005), implicating reorganization of the actin cytoskeleton in the CE process.

The planar cell polarity (PCP) pathway was defined through its control of hair cell orientation in the wing epithelium of *Drosophila* (Klein and Mlodzik, 2005). This pathway, termed the Wnt–PCP, β-catenin-independent or non-canonical pathway, uses universal Wnt-signalling components such as Frizzled (Fz) and Dishevelled (Dvl), but unlike the canonical Wnt pathway, involves components such as Strabismus, Prickle, Rho and Rac rather than glycogen synthase kinase-3, axin, and β-catenin (reviewed by Klein and Mlodzik, 2005; Wallingford and Habas, 2005). In *Xenopus*, inhibition or excessive activation of these components, for example, overexpression or dominant-negative forms of Fz-7 and Wnt11, inhibit CE (Djiane *et al*, 2000; Tada and Smith, 2000; Mlodzik, 2002). The signal generated through Wnt, Fz and Dvl results in the activation of RhoA and Rac1 in cultured cells and in *Xenopus* embryos, and activation of these small GTPases is required for CE (Habas *et al*, 2001, 2003; Tahinci and Symes, 2003). Dvl induces activation of Rho and Rac through two independent pathways. Rho activation requires the formin homology protein Daam-1 that binds to Dvl to mediate Wnt-induced Dvl–RhoA complex formation, and is essential for CE (Habas *et al*, 2001). Activation of Rho and Rac regulates changes in the actin cytoskeleton required for cell shape changes and migration (Hall, 1998), and Rho and Rac have both distinct and overlapping functions in CE (Tahinci and Symes, 2003; Ren *et al*, 2006). These small GTPases function as bimolecular switches and exist in a GDP-bound inactive form, and a GTP-bound active form that interacts with effector proteins to trigger multiple cellular responses, notably the rearrangement of the actin cytoskeleton inducing changes in cell shape and motility. Rho-associated kinase-α (Rok) functions downstream of RhoA in the Wnt–PCP pathway in the regulation of the actin cytoskeleton in *Drosophila* and in CE in *Xenopus* (Winter *et al*, 2001; Kim and Han, 2005). Although the outlines of the Wnt–PCP pathway have become clearer, the mechanism of Rho activation within this pathway has remained unresolved because neither Dvl nor Daam-1 can directly mediate the GDP–GTP exchange reaction.

Activation of small GTPases depends on the members of the Dbl-related guanine nucleotide-exchange factor (GEF) family that catalyse the GDP–GTP exchange reaction and

*Corresponding author. Laboratory of Molecular Genetics, National Institute of Child Health and Human Development, National Institutes of Health, 9000 Rockville Pike, Bethesda, MD 20892, USA.
Tel.: +1 301 496 4448; Fax: +1 301 496 0243;
E-mail: idawid@mail.nih.gov

Received: 15 August 2007; accepted: 10 January 2008; published online: 7 February 2008

are encoded by around 70 genes in humans (Rossman *et al*, 2005). The Dbl-related GEFs contain tandem Dapple homology (DH) and Ephexin–Pleckstrin homology (PH) domains; the DH domain is considered to be the catalytic centre for the exchange reaction (Liu *et al*, 1998; Rossman *et al*, 2005). Several GEFs such as *Quotto/Solo*, *Lfc* and *NET* have been suggested previously as candidates for mediating Rho or Rac activation in CE in *Xenopus* or zebrafish (Daggett *et al*, 2004; Miyakoshi *et al*, 2004; Kwan and Kirschner, 2005; Tse *et al*, 2005). Injection of an morpholino oligonucleotide (MO) against *Quotto* or of a dominant-negative form of *NET* inhibits gastrulation movements (Daggett *et al*, 2004; Miyakoshi *et al*, 2004), and MO knockdown of *Lfc* abrogates the ability of nocodazole to inhibit CE (Kwan and Kirschner, 2005). However, these GEFs have not been connected to the upstream components that are able to activate RhoA, and are not localized at the cell membrane or in association with the actin cytoskeleton (Miyakoshi *et al*, 2004; Kwan and Kirschner, 2005; Tse *et al*, 2005), and thus their role in Wnt–PCP-mediated CE remains unresolved.

In studies of the molecular mechanisms of CE, we screened for genes differentially expressed in the notochord of the *Xenopus* embryo by microarray analysis, as notochord cells undergo active CE. One of the genes discovered in this screen encodes a GEF with sequence similarity to human weak-similarity GEF (*WGEF*). We find that *WGEF* functions within the Wnt–PCP pathway, and can interact physically with Dvl and Daam-1, and depletion of *Xenopus WGEF* (*XWGEF*) resulted in axis elongation defects and inhibition of CE. Our data indicate that XWGEF mediates Wnt–PCP signalling in the regulation of cell movements during gastrulation.

Results

Isolation of WGEF as a gene preferentially expressed in the notochord

We screened for differentially expressed genes in the developing notochord using an Affymetrix microarray system that examines the expression of about 14 000 genes in *Xenopus laevis*. At late gastrula, when CE is active, we dissected four regions from the embryo, anterior mesoderm, posterior mesoderm, notochord and presomitic mesoderm. We generated expression profiles for these four regions and whole-sibling embryos (experiment, raw and processed data in ArrayExpress; www.ebi.ac.uk/arrayexpress; accession number, E-MEXP-717). Three types of comparison were carried out to generate a list of predominantly notochord-expressed genes: (1) posterior mesoderm versus anterior mesoderm; notochord genes are expected to be increased, as the notochord is located in the posterior mesoderm (Supplementary Figure S1); (2) posterior mesoderm versus whole embryo; notochord genes are expected to be increased (Supplementary Figure S1); and (3) notochord versus presomitic mesoderm. This comparison subdivided the group of posterior mesodermal genes identified in (1) and (2) (Supplementary Figure S2). Among the 388 probe sets that met these criteria (Supplementary Figure S2), we found several genes known to be expressed preferentially in the notochord (Supplementary Figure S3). We next carried out whole-mount *in situ* hybridization (WISH) with some of the previously uncharacterized notochord candidate genes. Among these, expressed sequence tag clone IMAGE: 5543566, which encodes a protein similar to human WGEF (hWGEF) (Wang *et al*, 2004), showed notochord expression (Figure 1D and E). We cloned the full-length cDNA by 5′ rapid amplification of cDNA ends (RACE), and found that it encodes a protein that shares 53% identity with hWGEF; similar sequences were found in the mouse and zebrafish (Figure 1A). These clones contain DH and PH domains and a C-terminal SH3 domain, and show higher sequence similarity among each other than to any other GEF; thus, we named our clone *XWGEF*. Reverse transcriptase–polymerase chain reaction (RT–PCR) analysis indicates that *XWGEF* expression begins at early gastrula stage and continues at a similar level through tadpole stages (Figure 1B). *In situ* hybridization and analysis of RNA from dissected embryos showed that *XWGEF* is expressed widely at the gastrula stage in animal and marginal regions (Figure 1C and F), becomes gradually restricted to the developing notochord at the end of the gastrulation (Figure 1D) and then shows preferential expression in the notochord throughout neurula stages (data not shown). At tail-bud stages, *XWGEF* transcripts were observed in the notochord and also in the head region (Figure 1E).

We next examined the subcellular localization of XWGEF in *Xenopus* embryos. Flag-tagged XWGEF protein was detected preferentially at the cell membrane, and it colocalized with actin as visualized by Texas Red-conjugated phalloidin (Figure 1G–G″). We noted that actin-rich protrusive structures showed strong colocalization of actin and XWGEF (Figure 1G″). Furthermore, green-fluorescent protein (GFP)-tagged XWGEF protein was detected using live imaging (Figure 1H and I). In animal cap cells from gastrula stage, XWGEF was found preferentially at the cell membrane outlined by membrane-tethered red-fluorescent protein (mtRFP) or adjacent to it (Figure 1H–H″). We also examined XWGEF localization in dorsal mesodermal cells, which undergo CE movements. GFP-tagged XWGEF protein was detected at or adjacent to the cell membrane (Figure 1I–I″), whereas mtRFP outlined the bipolar cell shape that cells assume in this tissue (Figure 1I′). These results suggest that XWGEF is associated with the plasma membrane in the *Xenopus* embryo.

Overexpression of WGEF activates RhoA

A previous report indicated that human WGEF is a strong activator of RhoA and a less effective activator of Rac1 and Cdc42 (Wang *et al*, 2004). We examined the activity of human and XWGEF in the activation of these GTPases, using pull-down assays with glutathione-*S*-transferase (GST) fusions of the Rhotekin Rho-binding domain (RBD) to detect RhoA–GTP and the GST fusion with the PAK-1-binding domain (PBD) for Rac1–GTP and Cdc42–GTP (Benard *et al*, 1999; Ren *et al*, 1999). Flag-tagged hWGEF, XWGEF, a deletion construct of hWGEF lacking most of the DH–PH domain (hWGEFΔGEF) and Ephexin as a GEF for all three GTPases (Shamah *et al*, 2001) were transfected into 293T cells and cultured for 24 h. Expression of hWGEF and XWGEF increased the level of active RhoA, whereas expression of hWGEFΔGEF did not (Figure 2A). To assay for the activation of Rac and Cdc42, their background activation levels were reduced by lowering the serum concentration in the medium (Habas *et al*, 2003). Under these conditions, we find that hWGEF and XWGEF did not activate Rac or Cdc42 above control levels, whereas Ephexin did (Figure 2B).

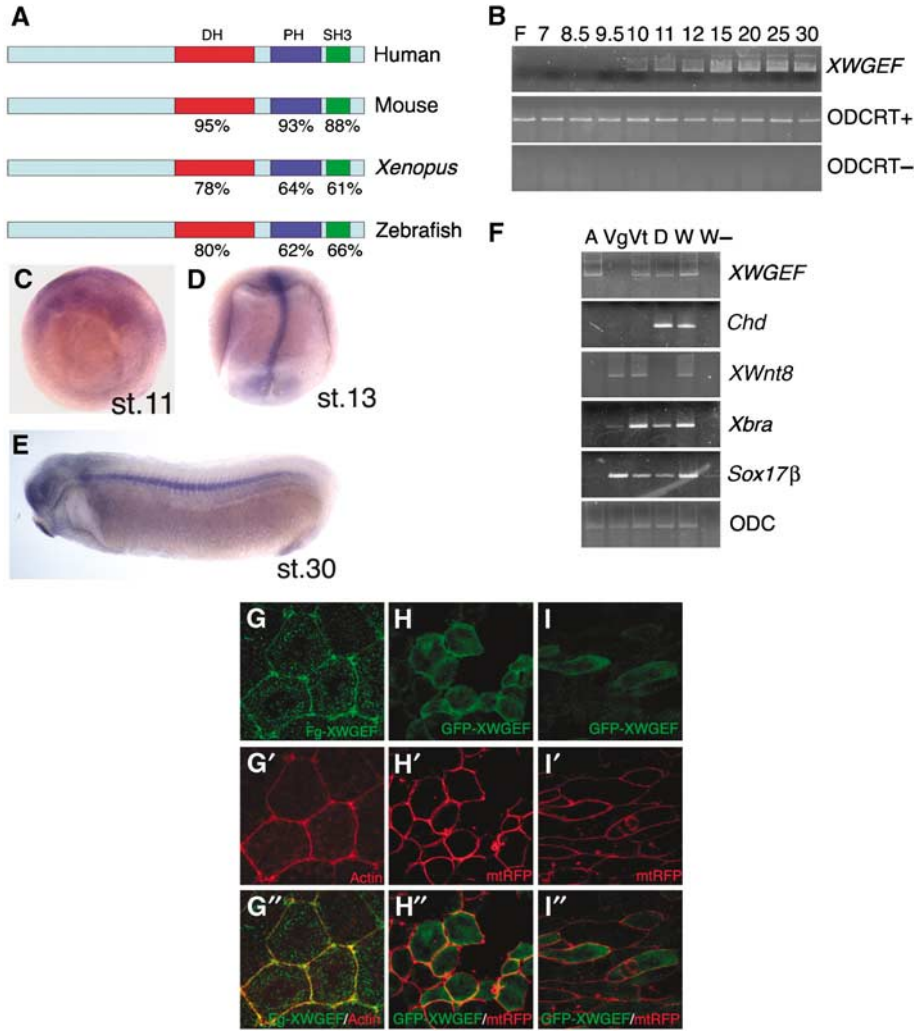

Figure 1 Molecular cloning and expression pattern of *XWGEF*. (**A**) Amino-acid sequence comparison of WGEF proteins. The DH, PH and SH3 domains of hWGEF (BC040640) share high sequence identity with mouse (AAH60376, Rho GEF 19), *Xenopus* (DQ640641, this study) and zebrafish (XP_697662, predicted sequence of Rho GEF 19-related protein) proteins. (**B**) Developmental expression of *XWGEF*. RT–PCR analysis was performed at various stages as indicated (Nieuwkoop and Faber, 1956); F, fertilized eggs. (**C**–**E**) *In situ* hybridization with *XWGEF*. (C) Vegetal view of stage-11 embryo showing widespread expression. (D) Dorsal view of stage-13 embryo; preferential expression of *XWGEF* was detected in the notochord. (E) Lateral view of stage-30 embryo showing *XWGEF* expression in notochord and head region. (**F**) RT–PCR with RNA from dissected stage-10 gastrula: animal (A) and vegetal (Vg) regions, and ventral (Vt) and dorsal (D) marginal zone; *XWGEF* transcripts were present in animal and marginal regions. *Chd*, *Wnt8*, *Xbra* and *Sox17*β served as markers for dorsal mesoderm, ventral mesendoderm, entire mesoderm and endoderm, respectively. W, whole embryo; W–, whole embryo without reverse transcriptase. (**G**–**I**) XWGEF is preferentially localized at the plasma membrane. *Fg–XWGEF* mRNA (50 pg) or *GFP–XWGEF* (100 pg) and *mtRFP* (100 pg) mRNA were injected into animal (H) or dorsal blastomeres (G, I) of four-cell-stage embryos. (G–G″) Fg–XWGEF localization. Dorsal (so-called Keller) explants were dissected at stage 10, fixed at mid-gastrula stage and stained with anti-Flag antibody (G) and Texas Red-conjugated phalloidin to visualize F-actin (G′); merged image (G″). Most of *XWGEF* protein was at the plasma membrane and colocalized with actin. Staining of explants from uninjected embryos with anti-Flag antibody showed no specific staining (data not shown). (H, I) GFP–XWGEF localization. GFP signal was visualized in live explants at mid-gastrula in animal caps (H), or at early neurula in Keller explants (I). mtRFP outlined the cell membranes (H′, I′). The merged images are shown in (H″, I″). GFP–XWGEF showed preferential membrane localization.

We further examined the specificity of WGEF binding using GST fusion proteins of Rho, Rac and Cdc42. We found that hWGEF and XWGEF strongly co-precipitated with RhoA at a level comparable to Ephexin, whereas hWGEFΔGEF did not (Figure 2C). hWGEF but not XWGEF showed a very weak interaction with Rac-1, and neither WGEF bound to Cdc42. These results confirm that hWGEF and XWGEF primarily act as GEFs for Rho. RhoA activation by WGEF was also tested in *Xenopus* embryos. RBD pull-down assays showed that overexpression of hWGEF and XWGEF activated RhoA in the *Xenopus* ventral marginal zone (VMZ) at a high level (Figure 2D). Thus, WGEF is an effective Rho GEF in mammalian and amphibian cells.

To study the role of XWGEF *in vivo*, we injected *hWGEF* and *XWGEF* mRNA into the *Xenopus* embryo. Embryos injected into their dorsal side had reduced anterior structures and a short anterior–posterior axis, with clear dosage dependence in the severity of the effect (Figure 2F and G, compare with the LacZ control in E; Table I). The phenotype seen after injection of *WGEF* was similar to that elicited by constitutively active *RhoA* (*CARhoA*) mRNA (data not shown; Table I; Wunnenberg-Stapleton *et al*, 1999; Tahinci and Symes, 2003; Ren *et al*, 2006). Co-injection of dominant-negative *RhoA* (*dnRhoA*) with *hWGEF* or *XWGEF* led to partial rescue of the body axis (Figure 2H; Table I). Consistent with the fact that WGEF is a Rho–GEF, dominant-negative *Rac1* (*dnRac1*) did

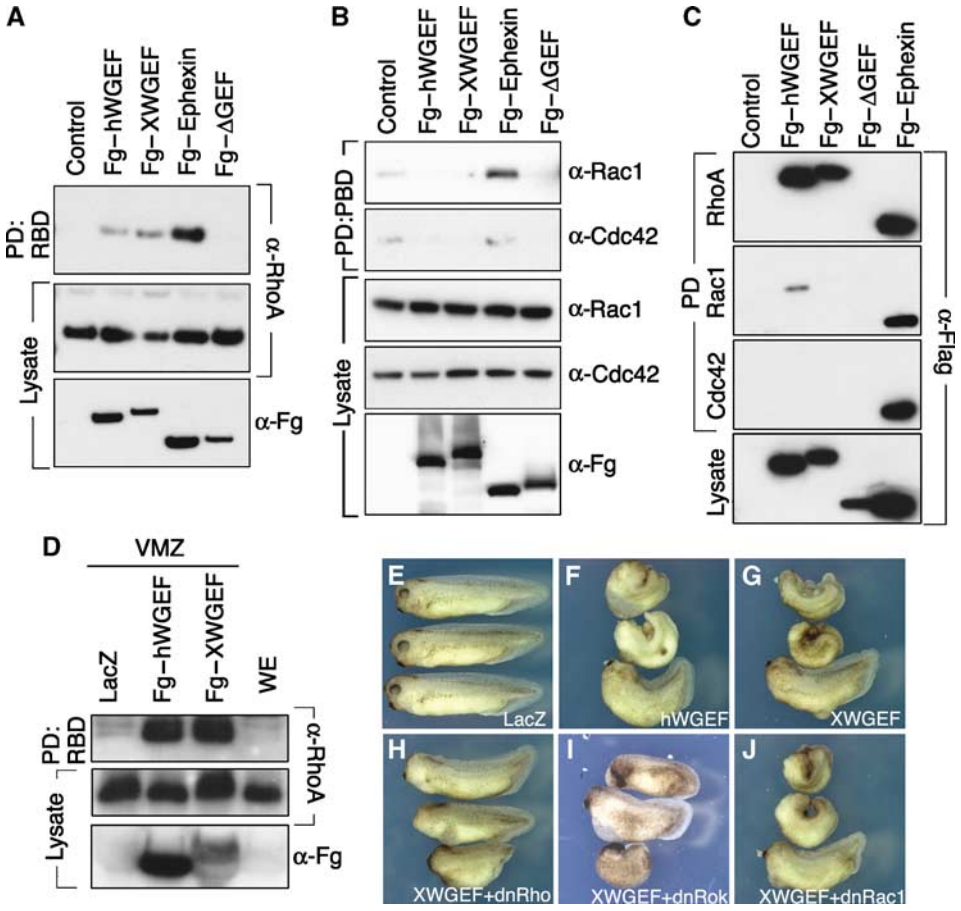

Figure 2 WGEF activates RhoA in cultured cells and *Xenopus* embryos. (**A**, **B**) hWGEF and XWGEF induce RhoA but not Rac1 and Cdc42 activation in HEK293T cells. Flag (Fg)-tagged hWGEF, XWGEF, Ephexin (positive control) and an inactive, DH domain-deleted form of hWGEF (ΔGEF; negative control) were transfected into HEK293T cells. Ephexin activates RhoA, Rac1 and Cdc42 (Shamah *et al*, 2001). (A) GTP–Rho was precipitated using RBD–GST and detected by anti-RhoA antibody. Endogenous RhoA and Flag-tagged GEF proteins in lysates were detected by anti-RhoA and anti-Flag antibody, respectively. (B) GTP-bound Rac1 and Cdc42 were precipitated by GST–PBD and detected by α-Rac1 and α-Cdc42 antibodies. (**C**) Fg–hWGEF and Fg–XWGEF bind to RhoA. Flag-tagged GEF constructs were transfected into the 293T cells, pulled down with GST–RhoA, Rac1 or Cdc42 and detected with Flag antibody. (**D**) WGEF activates RhoA in the *Xenopus* embryo. A 1-ng of *Fg–hWGEF* or *Fg–XWGEF* was injected into the ventral region of four-cell-stage embryos and VMZ was dissected at stage 10. (**E**–**H**) Overexpression of *WGEF* caused short body axis formation and suppression of head structures. mRNA was injected into the dorsal side of *Xenopus* embryos at the four-cell stage. (E) Injection of 250 pg of *lacZ*; (F) 250 pg of *Fg–hWGEF*; (G) 250 pg of *Fg–XWGEF*; (H) 250 pg of *Fg–XWGEF* and 500 pg of *dnRhoA* (hRhoAN19); (**I**) 250 pg of *Fg–XWGEF* and 500 pg of *dnRok*; (**J**) 250 pg of *Fg–XWGEF* and 500 pg of *dnRac1* (hRac1N17). Numbers of embryos are given in Table I.

not rescue the effect of WGEF (Figure 2J; Table I). Rok functions downstream of Rho in the regulation of CE (Kim and Han, 2005). Therefore, we tested whether dominant-negative Rok (dnRok) could rescue the effect of WGEF on axis formation. Co-injection of *dnRok* with *hWGEF* or *XWGEF* mRNA consistently led to substantial rescue of the phenotype (Figure 2I; Table I). These results indicate that WGEF modulates morphogenetic movements in the *Xenopus* embryo by activating the RhoA/Rok pathway.

XWGEF is required for CE in Xenopus

To study the role of *XWGEF* in early *Xenopus* development by a loss-of-function approach, we designed an antisense MO to deplete the endogenous *XWGEF* protein. XWGEF–MO efficiently blocked translation of *5′UTR–XWGEF–GFP* that contains the MO-target sequence (Supplementary Figure S4A and B). Although injection of 60 ng of control MO had no effect on development (Figure 3A), injection of 60 ng of XWGEF–MO into the dorsal marginal zone of the four-cell embryo resulted in embryos with short axis and small heads (Figure 3B). We also designed an MO for a splice-acceptor site of the *XWGEF* gene (XWGEF–ACMO) and confirmed the reduction of normal and the presence of mis-spliced *XWGEF* transcripts (Supplementary Figure S4C). Injection of XWGEF–ACMO into the dorsal marginal zone again resulted in embryos with shortened axes (Supplementary Figure S4D–H, 51/56 embryos). Both XWGEF–MO and XWGEF–ACMO cause neural tube-closure defects in severe cases, and induce stunted embryos with spina bifida (data not shown: 4/58 embryos for XWGEF–MO, 9/56 embryos for XWGEF–ACMO). WISH with mesodermal genes indicated that the developing notochord, marked by *Xnot*, *Chd* and the dorsal domain of *Xbra*, was broader and did not extend as far anteriorly in XWGEF–MO-injected embryos as in control MO-injected embryos, while the overall expression level of these genes was unaffected (Figure 3C–E and G–I). *Otx-2* expression, which marks anterior neuroectoderm and mesendoderm at this stage, also failed to localize properly in XWGEF–MO-injected

Table I Overexpression of hWGEF and XWGEF constructs induces anterior truncation with CE defects

mRNA (per embryo)[a]	Normal	Class I	Class II	Total	*P*-value[b]
1. LacZ (250 pg)	80	0	0	80	—
2. Fg–hWGEF (10 pg)	76	0	4	80	—
3. Fg–hWGEF (100 pg)	0	36	45	81	1.2E–17 (1)
4. Fg–hWGEF (250 pg)	0	14	69	83	7.1E–32 (1)
5. Fg–XWGEF (250 pg)	0	9	71	80	1.5E–35 (1)
6. Fg–hWGEF (250 pg) + dnRhoA (500 pg)	0	23	30	53	8.8E–4 (4)
7. Fg–XWGEF (250 pg) + dnRhoA (500 pg)	4	31	24	59	1.6E–9 (5)
8. Fg–hWGEF (250 pg) + dnRok (500 pg)	0	34	36	70	2.9E–5 (4)
9. Fg–XWGEF (250 pg) + dnRok (500 pg)	12	40	27	79	4.8E–13 (5)
10. Fg–hWGEF (250 pg) + dnRac1 (500 pg)	0	5	68	73	0.084 (4)
11. Fg–XWGEF (250 pg) + dnRac1 (500 pg)	0	7	66	73	0.8 (5)
12. Fg–hWGEFΔN (10 pg)	0	38	23	61	4.2E–14 (2)
13. Fg–hWGEFΔN (100 pg)	0	3	61	64	3.7E–8 (3)
14. CARhoA (20 pg)	0	61	19	80	—
15. CARhoA (100 pg)	0	0	83	83	—

Abbreviations: CARhoA, constitutively active RhoA; CE, convergent extension; dn, dominant negative; Fg, Flag; GEF, guanine nucleotide-exchange factor; hWGEF, human weak-similarity GEF; hWGEFΔN, the N-terminus deleted form of WGEF; WGEF, weak-similarity GEF; XWGEF, *Xenopus* WGEF.
Class I: anterior truncation with moderately short axis; see the bottom embryo in Figure 2F and G.
Class II: anterior truncation with very short axis and open neural tube; the examples are the two top embryos in Figure 2F and G.
[a]mRNA was injected into both dorsal blastomeres of four-cell stage embryos.
[b]Statistical test was carried out using Fisher's test for reduction or induction of class II phenotypes, compared with the samples indicated in parentheses.

embryos (Figure 3F and J), indicating that impairment of head development might be connected to a defect in migration of anterior tissues.

The results presented above suggest a requirement for *XWGEF* in CE in the *Xenopus* gastrula. We further explored this possibility using Keller explants and activin-treated animal caps (Asashima *et al*, 1990; Keller, 1991). Both types of explant from XWGEF–MO-injected embryos did not elongate, whereas control MO-injected explants did (Figure 3K–P and U), supporting the view that depletion of XWGEF inhibits CE. This inhibition was significantly rescued in activin-treated animal caps by co-injection of the morpholino with 1–2 pg of *hWGEF* mRNA (Figure 3Q and U), supporting the specificity of the effect of the XWGEF–MO inhibition.

As our results suggested that WGEF functions mainly as a Rho GEF (Figure 2), we attempted to rescue XWGEF depletion by activating Rho independently in *Xenopus*. Animal cap assays showed that 1 pg of *CARhoA* yielded statistically significant rescue of the suppression of CE in XWGEF–MO-injected explants, whereas *CARac1* did not (Figure 3R, S and U). To further test the relationship of WGEF with the Rho branch of the Wnt–PCP pathway, we co-injected *Rok* with the XWGEF–MO, again achieving significant rescue of CE (Figure 3T and U). These results indicate that *XWGEF* functions upstream of Rho activation and Rok function in the signalling cascade that controls CE during *Xenopus* gastrulation.

WGEF functions in the Wnt–PCP pathway during CE

The activation of Rho in response to Wnt–PCP signalling is required for CE (Habas *et al*, 2001), and the results presented above suggest that *XWGEF* is a component of this signalling cascade. To test this hypothesis, we performed epistatic analyses using activin-treated animal caps to delineate where *WGEF* functions in the Wnt–PCP pathway. The injection of dominant-negative *Xwnt-11* (*dnXWnt-11*) or *Xdd1*, which are dominant-negative forms of *Xenopus* Wnt-11 and Dvl, is known to suppress CE (Sokol, 1996; Tada and Smith, 2000; Figure 4A–D). Dvl can rescue the inhibition of CE by dnXWnt-11 (Tada and Smith, 2000), indicating that dnXWnt-11 inhibits CE upstream of Dvl. Analogous to this, inhibition of CE in animal caps by dnXWnt-11 was substantially rescued by injection of *hWGEF* mRNA (Figure 4E and I). Rescue of *Xdd1*-injected animal caps by *hWGEF* was achieved at the same high frequency, but with a lower level of elongation than for *dnXWnt-11*-injected caps (Figure 4F and I). In contrast, no rescue was observed by the injection of *hWGEF* mRNA when CE was inhibited by expression of the N-terminal portion of *Daam-1* (*N-Daam-1*), a dominant-negative form of Daam-1 (Habas *et al*, 2001; Figure 4G–I). We interpret these findings to indicate that XWGEF is a component of the Wnt–PCP pathway that functions downstream of the ligand. As shown below, XWGEF is a component of a complex that involves Dvl and Daam-1, explaining why XWGEF is less effective in rescuing the inhibition of CE by Xdd1 and ineffective in rescuing inhibition by N-Daam-1.

WGEF interacts with Dvl in Wnt-mediated Rho activation

In vivo experiments suggest that WGEF functions in the activation of Rho in response to Wnt signaling. This is supported by the fact that depletion of WGEF with the aid of RNA interference (RNAi) attenuates Rho activation in response to Wnt-1 (Figure 5B; Supplementary Figure S5). To further explore the mechanism of *WGEF*'s function, we examined the interactions between WGEF and the components of the Wnt–PCP pathway (Figure 5A). Co-immunoprecipitation experiments showed that mouse Dvl-2 (mDvl-2) interacts with hWGEF but not Ephexin (Figure 5C, lanes 3 and 4). Similarly, mDvl-2 interacted with XWGEF, and *Xenopus* Dvl (XDsh) co-immunoprecipitated with both XWGEF and hWGEF (Supplementary Figure S6B). The activation of Rho signalling requires the PDZ and DEP domains of mDvl-2, but the DIX domain is dispensable (Habas *et al*, 2001). We found that WGEF bound to ΔDIX–mDvl-2 but not to DIX–mDvl-2 (Figure 5C, lanes 5 and 6). The PDZ domain of mDvl-2 was co-immunoprecipitated with hWGEF, but the

DEP domain was not (Figure 5C, lanes 7 and 8). These results indicate that Dvl interacts with WGEF through the PDZ domain. We found that XWGEF bound to Xdd1, which is a partial deletion mutant of the PDZ domain, but the interaction was weaker than with wild-type XDsh (Supplementary Figure S6A and B). This result might reflect multiple sites of interaction between Dvl and WGEF, and is supported by a low but detectable level of interaction between WGEF and XDshN317T, a mutant that abrogates binding of Dsh to Dapper (Cheyette *et al*, 2002; Supplementary Figure S6C). Furthermore, WGEF co-immunoprecipitated with N-Daam-1 but not with the C-terminal portion, C-Daam-1 (Figure 5D, lanes 5 and 6). This binding was specific to WGEF because Ephexin did not bind to N-Daam-1 or C-Daam-1 (Figure 5C, lane 4; D lanes 7 and 8). As Daam-1 is known to bind to Dvl through its C-terminal portion (Habas *et al*, 2001), these results suggest that WGEF and Dvl-2 bind to different regions within Daam-1. Interestingly, the binding of hWGEF to mDvl-2 could be inhibited by N-Daam-1, which itself binds to WGEF (Figure 5E). This feature might explain the fact that N-Daam-1 functions as a dominant-negative form of Daam-1 (Habas *et al*, 2001). Thus, our results indicate that WGEF physically interacts with the Wnt–PCP pathway components Dvl and Daam-1.

If Wnt signalling involves Dvl–WGEF binding, we expect that these molecules colocalize after stimulation of the pathway. As XDsh localization can be regulated by *Xenopus* Fz 7 (Xfz-7) (Medina and Steinbeisser, 2000), we checked whether Xfz-7 regulates the colocalization of XDsh and XWGEF. In animal cap cells, XWGEF showed preferential localization at the plasma membrane in the absence or presence of XFz-7 (Figures 1H and 5F), whereas XDsh was re-localized to the membrane by injecting *XFz-7* mRNA (Medina and Steinbeisser, 2000; Figure 5F′ and G′), leading to colocalization of XWGEF and XDsh (Figure 5F″ and G″). We conclude that Fz activation of the Wnt–PCP pathway induces the colocalization of XWGEF and XDsh at the plasma membrane.

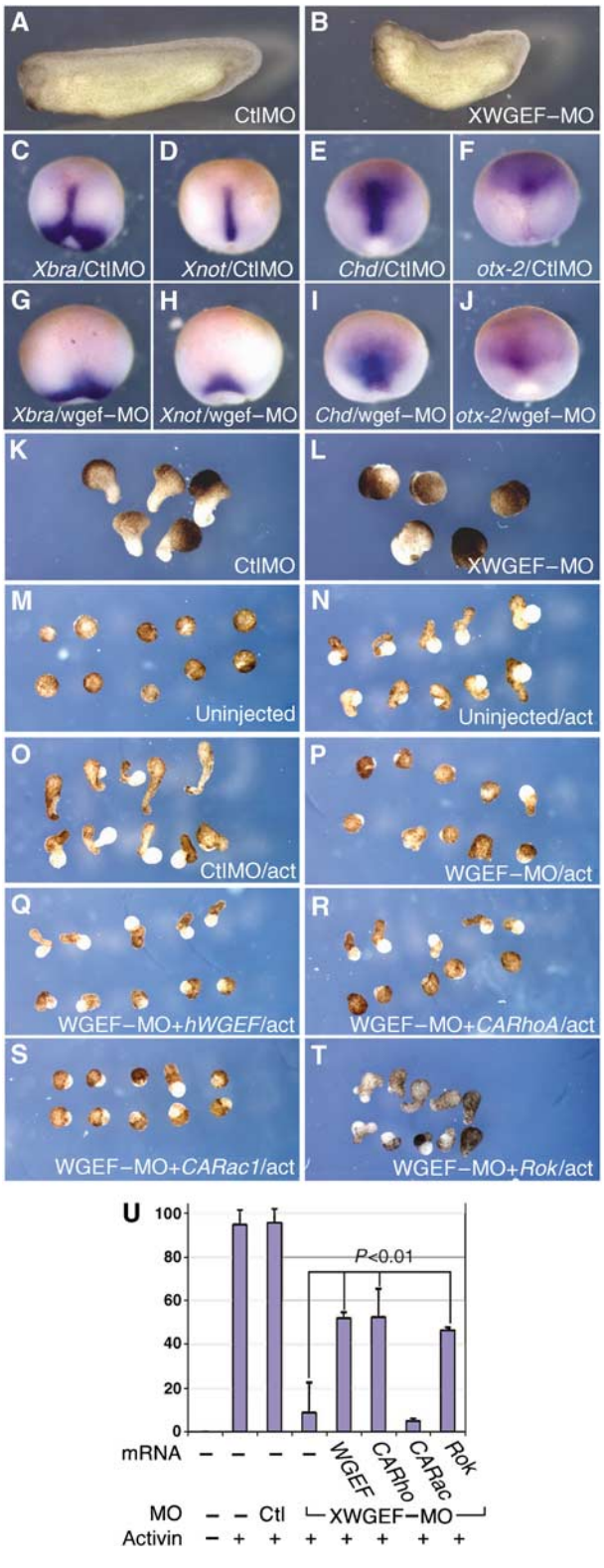

Figure 3 Depletion of *XWGEF* suppressed CE movements. (**A**, **B**) XWGEF–MO suppressed axis elongation. Sixty nanograms of control MO (CtlMO) (A) or XWGEF–MO (B) were injected into dorsal blastomeres at the four-cell stage. XWGEF–MO-injected embryos showed shortened axis (58/62 embryos), whereas CtlMO-injected embryos did not shows shortened axis (0/57). (**C**–**J**) XWGEF–MO suppressed elongation of the notochord, but did not inhibit mesodermal marker expression. Sixty nanograms of CtlMO (C–F) or XWGEF–MO (G–J) were injected into dorsal blastomeres at the four-cell stage together with *lacZ* RNA to mark the site of injection (red). WISH is shown for *Xbra* (C, G), *Xnot* (D, H), *Chd* (E, I), and *Otx-2* (F, J) at stage 13. (**K**, **L**) Keller sandwich explants from MO-injected embryos. Two dorsal sectors were dissected from stage-10 embryos and combined with each other. Explants injected with 60 ng of CtlMO extended (K, 42/50), whereas explants injected with 60 ng of XWGEF–MO did not extend (L, 4/41). The difference is statistically significant ($P = 3 \times E{-}13$; Supplementary Table S1). (**M**–**T**) XWGEF–MO inhibited CE in activin-treated animal caps, and this inhibition was rescued by expression of *hWGEF*, *CARhoA* or *Rok*. MOs with or without mRNA were injected into the animal region at the four-cell stage. Animal caps were dissected at stage 9, treated with activin for 3 h and photographed when sibling embryos reached stage 20. No elongation was seen without activin (M, 0/70 explants elongated), but elongation was induced by activin in uninjected (N, 73/77) or CtlMO-injected (60 ng) explants (O, 62/65). Injection of XWGEF–MO (60 ng) inhibited elongation (P, 7/80 elongated), which was rescued by co-injection of 1 or 2 pg of *hWGEF* mRNA (Q, 43/83), 1 pg of *CARhoA* mRNA (R, 33/63) or 50 pg of *Rok* mRNA (T, 19/41), but not *CARac1* mRNA (S, 2/61). (**U**) Bar graph showing the percentage of elongated animal caps in the experiments shown in panels M–T. Standard error bars are shown. Co-injection of *WGEF*, *CARho* and *Rok* mRNA showed statistically significant rescue compared with explants injected with XWGEF–MO alone ($P < 0.01$; Supplementary Table S1).

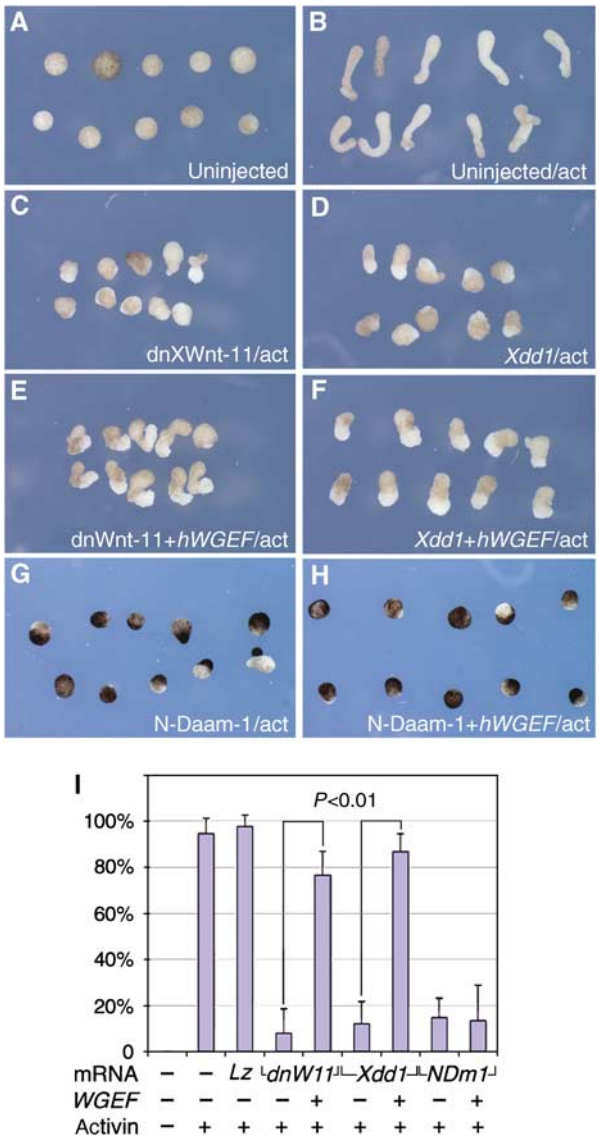

Figure 4 *WGEF* acts within the Wnt–PCP pathway. mRNAs were injected into the animal region at the four-cell stage, animal caps were dissected at stage 9, treated with activin and elongation was observed at equivalent stage 20. Animal caps did not elongate without activin (**A**, 0/54), but did so after activin treatment (**B**, 102/108). Injection of 1 ng of *dnXWnt-11* (**C**, 4/49) or *Xdd1* (**D**, 5/41) mRNA suppressed elongation, whereas *lacZ* did not suppress elongation (data not shown; 41/42). (**E**) Inhibition by *dnXWnt-11* was rescued by co-injection of 20 pg of *hWGEF* mRNA (52/68), but inhibition by *Xdd1* was only partially rescued (**F**, 39/45 explants elongated to a lesser extent). (**G**) *N-Daam-1* (2 ng mRNA) inhibited CE (G; 7/47) and 20 pg of *hWGEF* mRNA failed to rescue this inhibition (**H**, 7/52). (**I**) Bar graph showing the percentage of elongated animal caps in the experiments shown in panels A–H. Standard error bars are shown. $P<0.01$ for both comparisons (Supplementary Table S1).

Deletion of the Dvl-binding domain generates hyperactive WGEF

WGEF binds Dvl, a key molecule in Wnt signal transmission. Therefore, we sought to map the binding domain in WGEF involved in this interaction, using the deletion constructs shown in Figure 6A. We found that hWGEFΔN and hWGEFDH–PH could not bind Dvl, whereas the other mutants tested, in particular the N-terminal domain itself, retained binding activity (Figure 6A and B). This result indicates that the N-terminal portion of hWGEF is responsible for Dvl binding, and that Dvl and RhoA bind at different sites of WGEF, as hWGEFΔGEF, which retains the N-terminal domain, does not bind to RhoA (Figure 2C). To investigate the function of the N-terminal domain of WGEF, we tested the Rho activation activity of hWGEFΔN in 293T cells and in *Xenopus* embryos. Under comparable conditions, hWGEFΔN was more effective in RhoA activation in 293T cells than wild-type hWGEF (Figure 6C), and overexpression of *hWGEFΔN* or *XWGEFΔN* in *Xenopus* embryos activated RhoA at low doses at which wild-type *WGEF* was ineffective (Figure 6D). This increased activity caused by the deletion of the N-terminus may be accounted for by a conformational change in the remaining part of the molecule, affecting RhoA binding. We tested this prediction by analysing the binding affinity of the full length and ΔN forms of WGEF for RhoA, using *in vitro* synthesized proteins. hWGEFΔN showed substantially higher RhoA-binding activity than wild-type hWGEF (Figure 6E), suggesting that access of RhoA to its binding domain (PDZ domain) is restricted by the Dvl-binding domain (N-terminus) of WGEF. The increased activity of *WGEFΔN* was also apparent in observing phenotypic consequences in the embryo. Injection of 10 pg of *hWGEFΔN* mRNA was at least as effective in inducing anterior deficiencies and short axis as 100 pg of wild-type RNA, and 100 pg of the deletion construct generated very severe malformations in the embryos (Figure 6F–J; Table I). These results suggest that the N-terminal domain of WGEF has an autoinhibitory function, which may be released by Dvl binding.

Discussion

Several studies have demonstrated that the β-catenin-independent Wnt–PCP pathway controls CE movements during vertebrate development (Wallingford *et al*, 2002), and that activation of Rho is an indispensable step in this process (Habas *et al*, 2001; Tahinci and Symes, 2003). Thus, at least one GEF should be involved in the Rho activation step. Our results identify *WGEF* as a factor that mediates Rho activation in Wnt–PCP signalling during CE in *Xenopus*.

WGEF is a Rho–GEF required for CE

Rho class GTPases regulate rearrangements of the actin cytoskeleton to control cell morphology, motility and adhesion (Nobes and Hall, 1995; Hall, 1998). During axis formation, dorsal mesodermal cells are highly motile, a process in which active RhoA and Rac1 have distinct important functions (Tahinci and Symes, 2003; Ren *et al*, 2006). We propose that WGEF is a necessary component in the pathway that connects Wnt signalling to Rho activation in CE. WGEF morphant embryos showed a typical CE phenotype, which is less severe than that of embryos with a complete block of Rho activation (Tahinci and Symes, 2003), but elongation of animal caps treated with activin was suppressed fully by WGEFMO. This difference may reflect the fact that notochord, somites and spinal cord coordinately converge and extend in the embryo (Keller, 2002). As cell behaviour in CE in neural and mesodermal tissue is similar but not identical (Elul *et al*, 1997), common but variant molecular mechanism may be involved in CE in different tissues. *XWGEF* is mainly

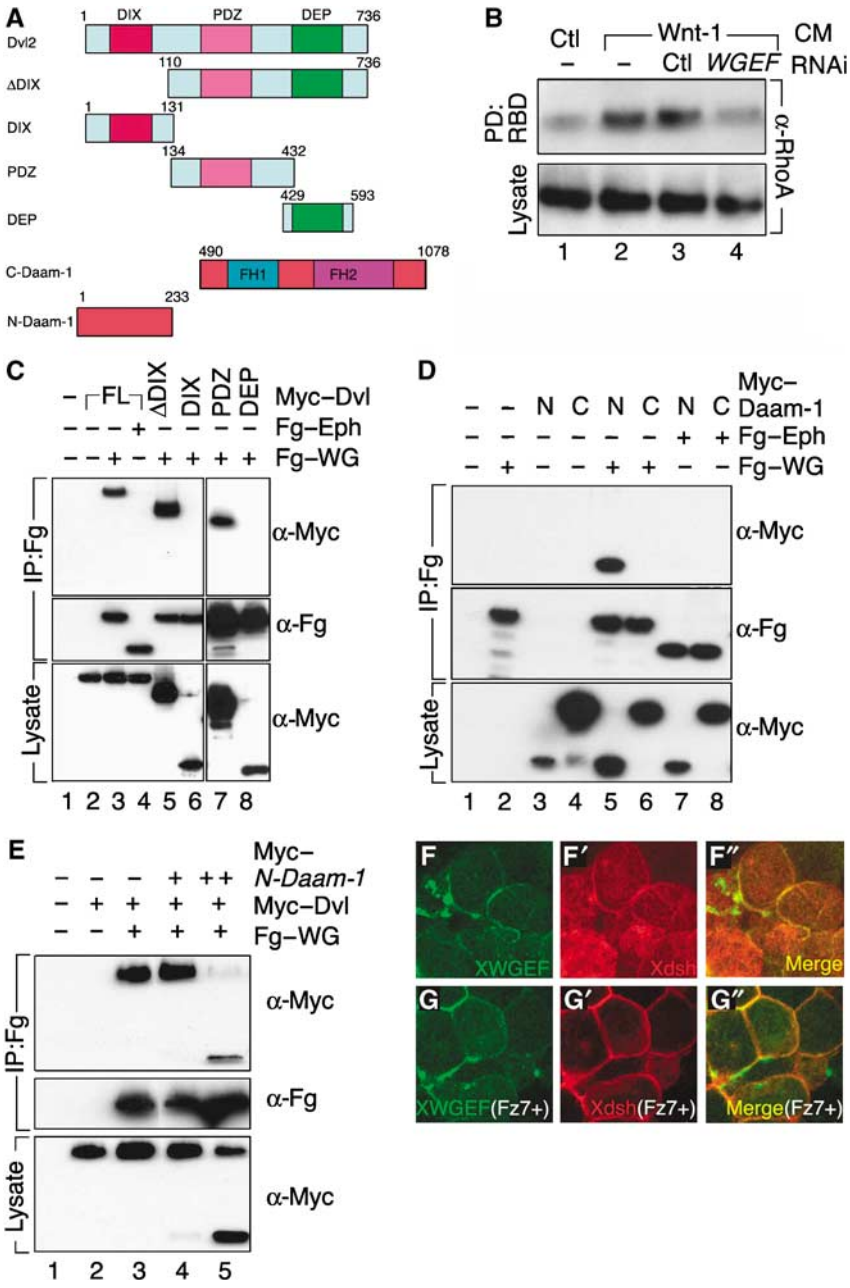

Figure 5 WGEF interacts with Wnt–PCP pathway components. (**A**) Schematic representation of epitope-tagged constructs of Dvl-2 and Daam-1. (**B**) Depletion of *hWGEF* blocks Rho activation by Wnt signaling. *hWGEF* or control (Ctl) RNAi was transfected into MCF-7 cells, and active RhoA was measured. Wnt-1-conditioned media (CM) stimulated the activation of RhoA (lane 2) as compared with Ctl CM (lane 1). Ctl RNAi had no effect (lane 3), but RNAi against *hWGEF* blocked the activation of Rho above control levels (lane 4). (**C**–**E**) In co-immunoprecipitation experiments, the antibodies used for precipitation are indicated by IP, and the antibodies used for blotting are shown on the right of each panel. (C) Dvl binds to hWGEF through its PDZ domain. Myc-tagged Dvl-2, Dvl-2ΔDIX and Dvl-2–PDZ co-precipitated with Fg–hWGEF (Fg–WG), but Myc–Dvl-2 did not bind to Fg–Ephexin (Fg–Eph). (D) Myc-tagged N-Daam-1 (N) but not C-Daam-1 (C) co-precipitated with Fg–WG, but neither co-precipitated with Fg–Eph. (E) Myc-tagged Dvl-2 binds to Fg–WG and this binding is abolished in a dose-dependent manner by cotransfection with Myc–*N-Daam-1*, a dominant-negative form of *Daam-1*. (**F**, **G**) Fz enhances the colocalization of Dsh and WGEF. *Fg–XWGEF* (50 pg) and *Myc–XDsh* (250 pg) mRNA was injected into the animal pole with (G) or without (F) 1 ng of *XFz-7* mRNA. Animal caps were dissected and stained with Flag (F, G) and Myc (F′, G′) antibody, and photographed using confocal microscopy. Merged images are shown in F″ and G″.

expressed in the notochord and may control its movements, which are the driving forces in activin-induced animal cap elongation, whereas other GEFs might contribute to CE in different tissues of the embryo.

WGEF is a component of the Wnt–PCP pathway

Five lines of evidence indicate that *WGEF* is a component of the Wnt–PCP pathway and functions in the control of CE: (1) WGEF is expressed in the notochord where CE is most active; (2) WGEF strongly and specifically activates RhoA (Figures 2 and 3); (3) WGEF functions downstream of Wnt ligand and Dvl, and upstream of RhoA and Rok in mediating CE (Figure 4); (4) Fz induces the colocalization of Dsh and WGEF, and depletion of endogenous WGEF inhibits Wnt-1-induced RhoA activation (Figure 5) and (5) WGEF binds to the PDZ domain of Dvl and to N-Daam-1 (Figure 5), and the

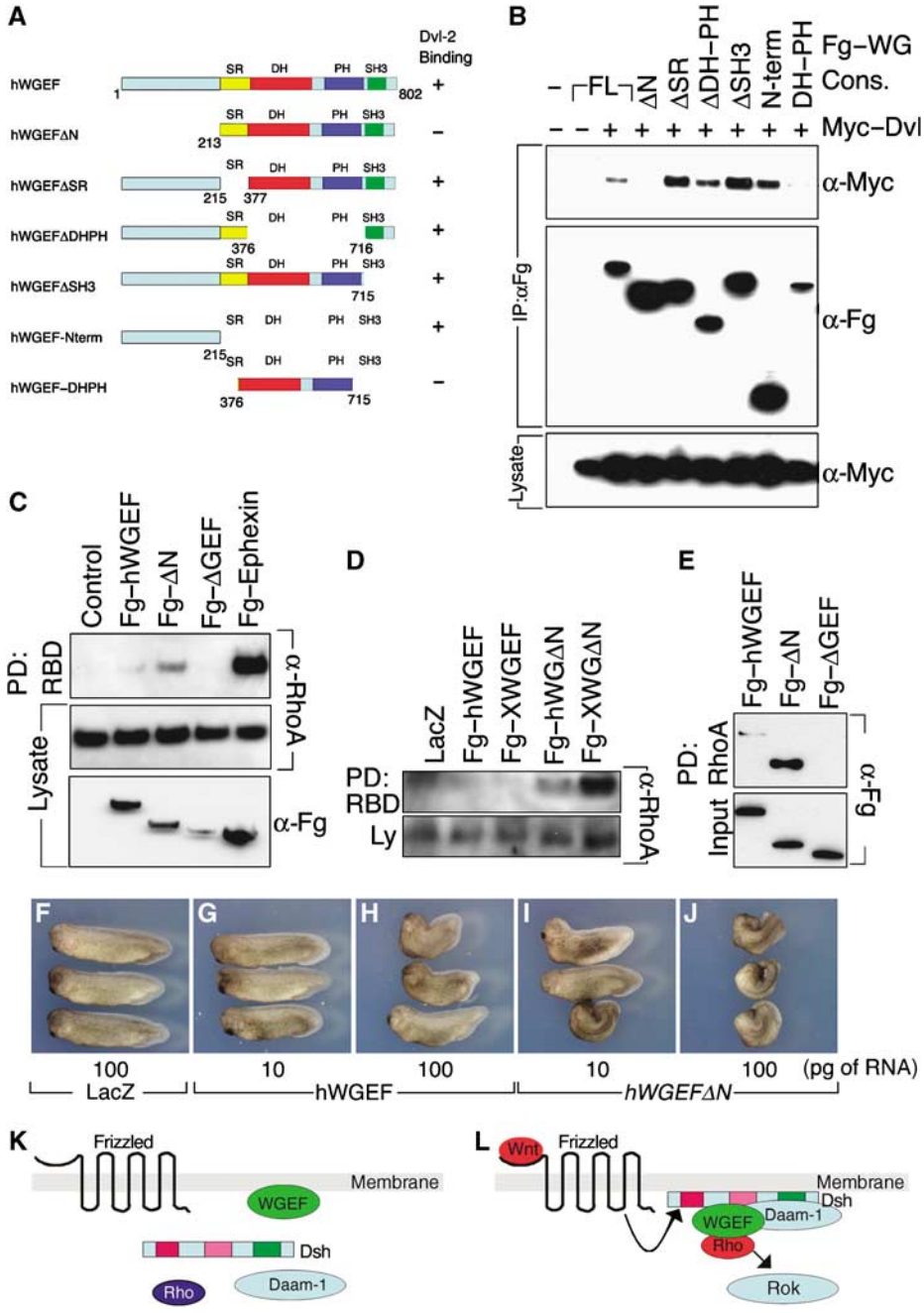

Figure 6 The N-terminal domain of hWGEF binds to Dvl and acts as an autoinhibitory domain. (**A**) Constructs of hWGEF, all of which were Flag tagged, and summary of Dvl binding. (**B**) Binding experiments were carried out after transfection into HEK293T cells. Antibodies used for blotting are indicated to the right of each panel. Only constructs that retain the N-terminal domain of hWGEF bind to Dvl-2. (**C**) Deletion of the Dvl-binding domain generates hyperactive WGEF. Constructs were transfected into HEK293T cells followed by assay for active RhoA. (**D**) WGEFΔN is more active than wild-type WGEF in Rho activation in the *Xenopus* embryo. Different constructs (100 pg of RNA) were injected into the VMZ at the four-cell stage, and dissected and assayed at stage 10. At these doses of injected RNA, wild-type hWGEF and XWGEF are not effective in Rho activation, but both N-terminal deletion (ΔN) constructs are strongly active. (**E**) The N-terminus deleted (ΔN) form of WGEF binds RhoA more effectively than the wild-type protein. *In vitro* translated *Fg–hWGEF*, *Fg–hWGEFΔN* and *Fg–hWGEFΔGEF* were tested by pull-down assay with RhoA–GST; *Fg–hWGEFΔGEF* is included as negative control. The ratio of Fg–hWGEFΔN to Fg–hWGEF binding to RhoA–GST was 3.9 ± 0.93; $n = 4$. (**F–J**) Overexpression of *WGEFΔN* is more effective than wild-type WGEF in the induction of embryonic defects. RNAs encoding the indicated constructs were injected into the dorsal side of *Xenopus* embryos at the four-cell stage; the amounts in picograms are indicated. Numbers of embryos are given in Table I. (**K**, **L**) A model for the interaction of Wnt–PCP components in regulating CE. (K) In the absence of Wnt signaling, Dvl, Daam-1 and Rho are in the cytosol (Park *et al*, 2006; Kim and Han, 2007), whereas WGEF is present at the membrane; Rho is not active. (L) Upon Wnt signalling and Fz activation, Dvl, Daam-1 and Rho are recruited to the membrane (Park *et al*, 2006; Kim and Han, 2007) and come to be colocalized and complexed with WGEF, leading to Rho activation.

WGEF N-terminal region binds to Dvl (Figure 6). This domain analysis led us to predict and verify that WGEFΔN is hyperactive in Rho binding, Rho activation and in affecting CE. The correlation of these effects provides further evidence connecting WGEF to the Wnt–PCP pathway and the control of CE. Although Dvl is able to bind to a nucleus-localized Rho–GEF, XNET1 (Miyakoshi *et al*, 2004), Dvl and Daam-1-binding are not general properties of GEFs, as Ephexin,

which is very effective in RhoA activation, fails to bind either protein (Figure 5C). As activation of Rho by the Wnt–PCP pathway requires the Dvl PDZ domain and Daam-1 (Habas *et al*, 2001), WGEF participates in the expected molecular interactions to be a component of this pathway. As Wnt stimulation activates Rac as well as Rho (Habas *et al*, 2003), and WGEF has little or no ability to activate Rac1, we speculate that a distinct Rac-specific GEF is involved in addition to WGEF in Wnt–PCP-dependent regulation of CE. The Wnt–PCP pathway has an important function in organogenesis besides regulating CE. For example, double knockout mice for *dvl-1* and *dvl-2* show malformations of the auditory sensory organ, the cochlea (Wang *et al*, 2006). It will be interesting to investigate whether WGEF has an important function in this process.

The N-terminal domains of certain GEFs negatively regulate their activity (Schmidt and Hall, 2002). For example, autoinhibition in the Rac–GEF Vav is released by phosphorylation of its N-terminal region by Syk kinase (Crespo *et al*, 1997; Tybulewicz, 2005). We observed a similar negative regulation of WGEF by its N-terminal domain, as seen by the hyperactivity of the N-terminal truncation (Figure 6). As Dvl binds to the N-terminal domain of WGEF (Figure 6), we suggest that Dvl binding induces WGEF activation. This view is supported by the enhanced affinity of WGEFΔN for RhoA, suggesting that the N-terminal domain inhibits RhoA binding (Figure 6E).

Our results indicate that colocalization of Dvl and WGEF at the plasma membrane is enhanced by Fz overexpression (Figure 5F and G). Wnt-11 induces Fz-7 accumulation and recruitment of Dvl (Witzel *et al*, 2006), and membrane localization of Dvl is important for signal transduction and Rho activation during CE (Wallingford *et al*, 2000; Park *et al*, 2005). Further, β-arrestin 2 is essential for Daam-1 and RhoA membrane localization and for RhoA activation in the control of CE in *Xenopus* (Park *et al*, 2006; Kim and Han, 2007). We suggest that stimulation of the Wnt–PCP pathway leads to colocalization and binding of Daam-1, Dvl and WGEF, resulting in the formation of a membrane-proximal multi-protein complex that mediates the release of WGEF autoinhibition, leading to activation of Rho and the propagation of the signal that regulates CE in the *Xenopus* embryo (Figure 6K and L).

Materials and methods

Cloning of hWGEF and XWGEF

A human WGEF cDNA clone was obtained from American Type Culture Collection (ATCC) (IMAGE: 3447806), and the open reading frame (ORF) was amplified using PCR and cloned into pCS2$^+$ vector. Partial clones for XWGEF-A and B were obtained from ATCC (XWGEFA: IMAGE: 5543566, XWGEFB: IMAGE: 7977743). To obtain full-length cDNA, we carried out 5′ RACE (BD Biosciences), yielding the 5′ portion of *XWGEF-B*. The full-length *XWGEF* ORF sequence was deposited in GenBank (accession number, DQ640641). Appropriate fragments were cloned into PCS2$^+$ vector. For epitope tagging, *hWGEF* and *XWGEF* ORF were cloned into PCS2$^+$flag vector (PCS2$^+$*flag-hWGEF*, PCS2$^+$*flag-XWGEF*). The following deletion constructs were generated with the aid of PCR and sequence-verified: PCS2$^+$*flag-hWGEFΔGEF* (deleted 377L-659K; lacking most of the DH and PH domains), PCS2$^+$*flag-hWGEFΔN* (deleted 1M-213R), PCS2$^+$*flag-XWGEFΔN* (deleted 1M-245G), PCS2$^+$*flag-hWGEFΔSR* (deleted 216A-376K), PCS2$^+$*flag-hWGEFΔDH-PH* (deleted 377L-715E), PCS2$^+$*flag-hWGEFΔSH3* (deleted 716-802V), PCS2$^+$*flag-hWGEFN-term* (deleted 216A-802V) and PCS2$^+$*flag-hWGEFDH-PH* (containing 377L-715E plus three upstream Flag tags). *XWGEF5′UTR–GFP* was constructed by ligating XWGEF5′UTR plus start codon into pT7SP6-*GFP* vector. Detailed maps and construction data are available upon request.

Synthetic transcripts and Xenopus injections

Synthetic RNA was prepared using mMessage mMachine (Ambion). The plasmids used as mRNA templates are listed in Supplementary data. Four-cell *Xenopus* embryos were injected with 5 nl of capped RNA or MO in each of the two dorsal blastomeres. The embryos were cultured in 0.2XMMR. The sequence of XWGEF–MO is as follows: 5′-TCATTGTGTGAGTCCATCAGTCCCG-3′ (designed for translation initiation site) and 5′-GTATTCCTGATAGAGAATGGC TGGG-3′ (designed for splice-acceptor site). Gene Tool control MO was used as negative control (CtlMO 5′-CCTCTTACCTCAGTTAC AATTTATA-3′). Animal cap assays were carried out as previously described (Tanegashima *et al*, 2004). Keller explants were dissected from stage-10 embryos and cultured in Steinberg's solution supplemented with 0.1% bovine serum albumin. All injection and explant experiments were carried out at least three times. Statistical comparisons were done using Fisher's *t*-test.

WISH, LacZ staining and RT–PCR

WISH was carried out according to Harland (1991) using *Xbra* (Smith *et al*, 1991), *Chd* (Sasai *et al*, 1994), *Otx-2* (Pannese *et al*, 1995) and *Xnot* (von Dassow *et al*, 1993) as probes. PCS2$^+$*XWGEF* was linearized by *Eco*RI and transcribed by T7 polymerase to make antisense probe. For *XWGEF* staining, we cleared embryos using BABB after staining. RT–PCR and LacZ staining were performed as previously described (Tanegashima *et al*, 2004). The primer sequence of *Chd*, *Xbra*, *Xwnt8* and *Sox17*β were from the Dr De Robertis' homepage (http://www.hhmi.ucla.edu/derobertis/index.html), and that of *ODC* was obtained from XMMR (http://www.xenbase.org/WWW/Welcome.html). Primer set for *XWGEF* was the following: upper 5-GAGGTGCCGGGGGAGGTTTTC-3 and lower 5′-GGGGGCCCGTCGCTGTAGTT-3′.

Rho, Rac and Cdc42 activation and binding assays

Cultured human embryonic kidney (HEK)293T cells were transfected with pCS2$^+$*flag-hWGEF*, pCS2$^+$*flag-XWGEF*, pCS2$^+$*flag-hWGEFΔN*, pCS2$^+$*flag-hWGEFΔGEF* and pGL3$^+$*flag-rat-ephexin* (Shamah *et al*, 2001) using lipofectamine (Invitrogen) and lysed in Rho lysis buffer (Ren *et al*, 1999; Habas *et al*, 2001). For Rac/Cdc42 assays, cells were incubated in 0.5% serum 6 h prior to transfection, maintained in this serum concentration after transfection and lysed 24 h post transfection in lysis buffer for Rac/Cdc42 (Benard *et al*, 1999; Habas *et al*, 2003). For *in vitro* transcription-coupled translation, we used the TnT SP6 high-yield protein expression system (Promega), and purified the protein using CENTRISEP (Princeton Separations). *Xenopus* VMZ at stage 10.5 was lysed in Tris–HCl pH 7.2, 150 mM NaCl, 1% Triton X-100, 10 mM $MgCl_2$, cleared and 5 M NaCl was added to adjust the lysate to 500 mM. GST–RBD and GST–PBD-binding assays were performed as described (Habas *et al*, 2001, 2003) using anti-RhoA (26A4) (Santa Cruz), anti-Rac-1 (BD Biosciences), anti-Cdc42mAb (BD Biosciences) and anti-FlagM2 (Fg; Sigma) antibodies. Rho, Rac and Cdc42–GST were produced as described (Habas *et al*, 2001). Rho-, Rac- and Cdc42-binding assays were carried out in Tris–HCl pH 7.2, 200 mM NaCl, 1% Triton X-100 and 10 mM ethylenediamine tetraacetic acid.

Immunoprecipitation

HEK293T cells were transfected with pCS2$^+$*myc-dvl2*, pCS2$^+$ *myc-dvl2ΔDIX*, pCS2$^+$*myc-dvl2-DIX*, pCS2$^+$*myc-dvl2-PDZ*, pCS2$^+$*myc-dvl2-DEP*, pGL3-*flag-ephexin*, pCS2$^+$*N-Daam-1*, pCS2$^+$*C-Daam-1* (Habas *et al*, 2001), pCS2$^+$*flag-hWGEF*, pCS2$^+$*flag-XWGEF* and deletion construct of *fg-hWGEF* as described above, and lysed in 20 mM Tris–HCl (pH 7.5), 1% Triton, 150 mM NaCl and 1 × Proteinase inhibitor cocktail (Roche). Proteins were immunoprecipitated with rabbit anti-Flag polyclonal antibody (Sigma) and proteins were detected with anti-FlagM2 (Sigma) or anti-Myc (9E10; Santa Cruz) antibodies.

Wnt-1 treatment and RNAi transfection

MCF-7 cells cultured in six-well plates were transfected with 40 pmol of control RNAi (no. 4635; Ambion) or hWGEF RNAi

(no. 122068; Ambion) using lipofectamine RNAi MAX (Invitrogen), cultured for 84 h, the media was changed to 0.5% fetal bovine serum (FBS) in Dulbecco's modified Eagle's medium (DMEM) for 12 h and the cells were treated with Wnt-1 or control conditioned media for 3 h. Conditioned media were prepared from 293T cells transfected with pcdna3-*Wnt-1* or pcdna3 vector for 96 h in 0.5% FBS in DMEM.

Supplementary data

Supplementary data are available at *The EMBO Journal* Online (http://www.embojournal.org).

Acknowledgements

We thank Drs S Sokol, R Habas, M Greenberg, JC Smith, D Kimelman, RT Moon, BN Cheyette, GH Kim, JK Han, JS Gutkind and E Boncinelli for reagents; Raymond Habas for advice on Rho assays and for critical reading of the manuscript and members of the Dawid laboratory for stimulating discussions. KT especially thanks R Yagi for encouragement and support. This work was supported by the Intramural Research Program of the National Institute of Child Health and Human Development, National Institutes of Health, and was supported in part by a JSPS fellowship to KT.

References

Asashima M, Nakano H, Simada K, Ishii K, Shibai H, Ueno N (1990) Mesodermal induction in early amphibian embryos by activin A (erythroid differentiation factor). *Rouxs Arch Dev Biol* **198:** 330–335

Benard V, Bohl BP, Bokoch GM (1999) Characterization of rac and cdc42 activation in chemoattractant-stimulated human neutrophils using a novel assay for active GTPases. *J Biol Chem* **274:** 13198–13204

Cheyette BN, Waxman JS, Miller JR, Takemaru K, Sheldahl LC, Khlebtsova N, Fox EP, Earnest T, Moon RT (2002) Dapper, a dishevelled-associated antagonist of beta-catenin and JNK signaling, is required for notochord formation. *Dev Cell* **4:** 449–461

Copp AJ, Greene ND, Murdoch JN (2003) The genetic basis of mammalian neurulation. *Nat Rev Genet* **4:** 784–793

Crespo P, Schuebel KE, Ostrom AA, Gutkind JS, Bustelo XR (1997) Phosphotyrosine-dependent activation of Rac-1 GDP/GTP exchange by the vav proto-oncogene product. *Nature* **385:** 169–172

Daggett DF, Boyd CA, Gautier P, Bryson-Richardson RJ, Thisse C, Thisse B, Amacher SL, Currie PD (2004) Developmentally restricted actin-regulatory molecules control morphogenetic cell movements in the zebrafish gastrula. *Curr Biol* **14:** 1632–1638

Djiane A, Riou J, Umbhauer M, Boucaut J, Shi D (2000) Role of frizzled 7 in the regulation of convergent extension movements during gastrulation in *Xenopus laevis*. *Development* **127:** 3091–3100

Elul T, Koehl MA, Keller R (1997) Cellular mechanism underlying neural convergent extension in *Xenopus laevis* embryos. *Dev Biol* **191:** 243–258

Habas R, Dawid IB, He X (2003) Coactivation of Rac and Rho by Wnt/Frizzled signaling is required for vertebrate gastrulation. *Genes Dev* **17:** 295–309

Habas R, Kato Y, He X (2001) Wnt/Frizzled activation of Rho regulates vertebrate gastrulation and requires a novel Formin homology protein Daam1. *Cell* **107:** 843–854

Hall A (1998) Rho GTPases and the actin cytoskeleton. *Science* **279:** 509–514

Harland RM (1991) *In situ* hybridization: an improved whole-mount method for *Xenopus* embryos. *Methods Cell Biol* **36:** 685–695

Keller R (1991) Early embryonic development of *Xenopus laevis*. *Methods Cell Biol* **36:** 61–113

Keller R (2002) Shaping the vertebrate body plan by polarized embryonic cell movements. *Science* **298:** 1950–1954

Keller R, Jansa S (1992) *Xenopus* gastrulation without a blastocoel roof. *Dev Dyn* **195:** 162–176

Kim GH, Han JK (2005) JNK and ROKalpha function in the noncanonical Wnt/RhoA signaling pathway to regulate *Xenopus* convergent extension movements. *Dev Dyn* **232:** 958–968

Kim GH, Han JK (2007) Essential role for beta-arrestin 2 in the regulation of *Xenopus* convergent extension movements. *EMBO J* **26:** 2513–2526

Klein TJ, Mlodzik M (2005) Planar cell polarization: an emerging model points in the right direction. *Annu Rev Cell Dev Biol* **21:** 155–176

Kwan KM, Kirschner MW (2005) A microtubule-binding Rho–GEF controls cell morphology during convergent extension of *Xenopus laevis*. *Development* **132:** 4599–4610

Liu X, Wang H, Eberstadt M, Schnuchel A, Olejniczak ET, Meadows RP, Schkeryantz JM, Janowick DA, Harlan JE, Harris EA, Staunton DE, Fesik SW (1998) NMR structure and mutagenesis of the N-terminal Dbl homology domain of the nucleotide exchange factor Trio. *Cell* **95:** 269–277

Medina A, Steinbeisser H (2000) Interaction of Frizzled 7 and Dishevelled in *Xenopus*. *Dev Dyn* **218:** 671–680

Miyakoshi A, Ueno N, Kinoshita N (2004) Rho guanine nucleotide exchange factor xNET1 implicated in gastrulation movements during *Xenopus* development. *Differentiation* **72:** 48–55

Mlodzik M (2002) Planar cell polarization: do the same mechanisms regulate *Drosophila* tissue polarity and vertebrate gastrulation? *Trends Genet* **18:** 564–571

Nieuwkoop PD, Faber J (1956) *Normal Table of Xenopus laevis (Daudin)*. Amsterdam, the Netherlands: Elsevier North-Holland

Nobes CD, Hall A (1995) Rho, rac, and cdc42 GTPases regulate the assembly of multimolecular focal complexes associated with actin stress fibers, lamellipodia, and filopodia. *Cell* **81:** 53–62

Pannese M, Polo C, Andreazzoli M, Vignali R, Kablar B, Barsacchi G, Boncinelli E (1995) The *Xenopus* homologue of Otx2 is a maternal homeobox gene that demarcates and specifies anterior body regions. *Development* **121:** 707–720

Park E, Kim GH, Choi SC, Han JK (2006) Role of PKA as a negative regulator of PCP signaling pathway during *Xenopus* gastrulation movements. *Dev Biol* **292:** 344–357

Park TJ, Gray RS, Sato A, Habas R, Wallingford JB (2005) Subcellular localization and signaling properties of dishevelled in developing vertebrate embryos. *Curr Biol* **15:** 1039–1044

Ren R, Nagel M, Tahinci E, Winklbauer R, Symes K (2006) Migrating anterior mesoderm cells and intercalating trunk mesoderm cells have distinct responses to Rho and Rac during *Xenopus* gastrulation. *Dev Dyn* **235:** 1090–1099

Ren XD, Kiosses WB, Schwartz MA (1999) Regulation of the small GTP-binding protein Rho by cell adhesion and the cytoskeleton. *EMBO J* **18:** 578–585

Rossman KL, Der CJ, Sondek J (2005) GEF means go: turning on RHO GTPases with guanine nucleotide-exchange factors. *Nat Rev Mol Cell Biol* **6:** 167–180

Sasai Y, Lu B, Steinbeisser H, Geissert D, Gont LK, De Robertis EM (1994) *Xenopus* chordin: a novel dorsalizing factor activated by organizer-specific homeobox genes. *Cell* **79:** 779–790

Schmidt A, Hall A (2002) Guanine nucleotide exchange factors for Rho GTPases: turning on the switch. *Genes Dev* **16:** 1587–1609

Shamah SM, Lin MZ, Goldberg JL, Estrach S, Sahin M, Hu L, Bazalakova M, Neve RL, Corfas G, Debant A, Greenberg ME (2001) EphA receptors regulate growth cone dynamics through the novel guanine nucleotide exchange factor ephexin. *Cell* **105:** 233–244

Shih J, Keller R (1992) Cell motility driving mediolateral intercalation in explants of *Xenopus laevis*. *Development* **116:** 901–914

Smith JC, Price BM, Green JB, Weigel D, Herrmann BG (1991) Expression of a *Xenopus* homolog of Brachyury (T) is an immediate-early response to mesoderm induction. *Cell* **67:** 79–87

Sokol SY (1996) Analysis of Dishevelled signalling pathways during *Xenopus* development. *Curr Biol* **6:** 1456–1467

Tada M, Smith JC (2000) Xwnt11 is a target of *Xenopus* Brachyury: regulation of gastrulation movements via Dishevelled, but not through the canonical Wnt pathway. *Development* **127:** 2227–2238

Tahinci E, Symes K (2003) Distinct functions of Rho and Rac are required for convergent extension during *Xenopus* gastrulation. *Dev Biol* **259:** 318–335

Tanegashima K, Haramoto Y, Yokota C, Takahashi S, Asashima M (2004) Xantivin suppresses the activity of EGF-CFC genes to regulate nodal signaling. *Int J Dev Biol* **48:** 275–283

Tse SW, Broderick JA, Wei ML, Luo MH, Smith D, McCaffery P, Stamm S, Andreadis A (2005) Identification, expression analysis, genomic organization and cellular location of a novel protein with a RhoGEF domain. *Gene* **359:** 63–72

Tybulewicz VL (2005) Vav-family proteins in T-cell signalling. *Curr Opin Immunol* **17:** 267–274

von Dassow G, Schmidt JE, Kimelman D (1993) Induction of the *Xenopus* organizer: expression and regulation of Xnot, a novel FGF and activin-regulated homeo box gene. *Genes Dev* **7:** 355–366

Wallingford JB, Habas R (2005) The developmental biology of Dishevelled: an enigmatic protein governing cell fate and cell polarity. *Development* **132:** 4421–4436

Wallingford JB, Fraser SE, Harland RM (2002) Convergent extension: the molecular control of polarized cell movement during embryonic development. *Dev Cell* **2:** 695–706

Wallingford JB, Rowning BA, Vogeli KM, Rothbacher U, Fraser SE, Harland RM (2000) Dishevelled controls cell polarity during *Xenopus* gastrulation. *Nature* **405:** 81–85

Wang J, Hamblet NS, Mark S, Dickinson ME, Brinkman BC, Segil N, Fraser SE, Chen P, Wallingford JB, Wynshaw-Boris A (2006) Dishevelled genes mediate a conserved mammalian PCP pathway to regulate convergent extension during neurulation. *Development* **133:** 1767–1778

Wang Y, Suzuki H, Yokoo T, Tada-Iida K, Kihara R, Miura M, Watanabe K, Sone H, Shimano H, Toyoshima H, Yamada N (2004) WGEF is a novel RhoGEF expressed in intestine, liver, heart, and kidney. *Biochem Biophys Res Commun* **324:** 1053–1058

Winter CG, Wang B, Ballew A, Royou A, Karess R, Axelrod JD, Luo L (2001) *Drosophila* Rho-associated kinase (Drok) links Frizzled-mediated planar cell polarity signaling to the actin cytoskeleton. *Cell* **105:** 81–91

Witzel S, Zimyanin V, Carreira-Barbosa F, Tada M, Heisenberg CP (2006) Wnt11 controls cell contact persistence by local accumulation of Frizzled 7 at the plasma membrane. *J Cell Biol* **175:** 791–802

Wunnenberg-Stapleton K, Blitz IL, Hashimoto C, Cho KW (1999) Involvement of the small GTPases XRhoA and XRnd1 in cell adhesion and head formation in early *Xenopus* development. *Development* **126:** 5339–5351